Neutral sodium from comet Hale-Bopp: a third type of tail

G. Cremonese

Osservatorio Astronomico, Vic. Osservatorio 5, 35122 Padova – Italy

H. Boehnhardt¹

University of Munich, Scheinerstr. 1, D-81679 Munich – Germany

J. Crovisier and H. Rauer²

Observatoire de Paris-Meudon, 5 Place Jules Janssen, F-92195 Meudon - France

A. Fitzsimmons

Queen's University, Belfast, BT7 1NN – United Kingdom

M. Fulle

Osservatorio Astronomico, via Tiepolo 11, I-34131 Trieste-Italy

J. Licandro³

Instituto de Astrofisica de Canarias, Via Lactea s/n, 38200 La Laguna – Spain

D. Pollacco

Isaac Newton Group, Apartado de Correos 368, Santa Cruz de La Palma, 38780 Tenerife – Spain

G.P. Tozzi

Osservatorio Astrofisico di Arcetri, Largo E.Fermi 5, 50125 Firenze – Italy

and

R.M. West

ESO, Karl-Schwarzschild-Str. 2, D-85748 Garching - Germany

Received	_ ;	accepted
----------	------------	----------

¹ESO, Santiago del Cile

²Deutsche Forschungsanstalt für Luft und Raumfahrt, Institut für Planetenerkundung, D−12484 Berlin − Germany

³Dept. de Astronomia, Universidad de la República, Tristán Narvaja 1674, 11200 Montevideo – Uruguay

ABSTRACT

We report on the discovery and analysis of a striking neutral sodium gas tail associated with comet C/1995 O1 Hale-Bopp. Sodium D-line emission has been observed at heliocentric distance $r \leq 1.4$ AU in some long-period comets and the presence of neutral sodium in the tailward direction of a few bright comets has been noted, but the extent, and in particular the source, has never been clear. Here we describe the first observations and analysis of a neutral sodium gas tail in comet Hale-Bopp, entirely different from the previously known ion and dust tails. We show that the observed characteristics of this third type of tail are consistent with it being produced by radiation pressure due to resonance fluorescence of sodium atoms and that the lifetime for photoionization is consistent with recent theoretical calculations.

Subject headings: comets: general — comets: individual (Hale-Bopp 1995 O1) — atomic processes — scattering

1. Introduction

Sodium emission has been previously observed in both long-period and dynamically new comets (Rahe et al. 1976, Sivaraman et al. 1979, Hicks and Fink 1997). Although the abundance of sodium in comets is much lower than other observable elements and molecules, it can be used as a tracer of processes acting in the same environment. This is because the extremely high efficiency of the sodium atom in resonant scattering of solar radiation makes it detectable even when the column density is low. For instance the absolute sodium abundance in the Io atmosphere is ~1%, yet it has been the neutral species most studied after its discovery and is an important tracer of the atmospheric interactions with the plasma torus (Thomas 1992). Further examples are that of the tenuous atmospheres of Mercury and the Moon. If the sources of the sodium observed in comet Hale-Bopp and in other comets can be identified, it could be possible to study the sodium distribution and dynamics as a tracer of physical processes that may otherwise not be easily detectable.

In the context of the present observations, the first possible identification of a sodium tail was recorded by Newall (1910) during the spectroscopic observation of comet C/1910 A1, made with a direct-vision prism inserted between the eye and the eyepiece of the 25-inch telescope. Later a 7 degree-long sodium tail was reported in comet C/1957 P1 Mrkos by Nguyen-Huu-Doan (1960) using a Schmidt camera with an objective prism. In both cases the sodium tail was identified through spectroscopic observation of the D-line emission, however there was no detailed analysis of the morphology of the tail and the mechanism responsible for these features. More recently, sodium was observed in comets C/1965f Ikeya-Seki (Spinrad and Miner, 1968, Huebner, 1970), C/1969 Y1 Bennett (Rahe et al. 1976) and C/1976 V1 West (Sivaraman et al. 1979) within 100000 km of the nucleus. The Giotto spacecraft performed in-situ measurements in the coma of comet Halley and found the ratio Na/O = 4.9×10^{-3} , close to the cosmic ratio (Jessberger and Kissel, 1991). In this letter we report on the discovery and analysis of an extensive neutral sodium tail observed in comet C/1995 O1 Hale-Bopp, first reported by Cremonese (1997).

2. Observations and data reduction

Images of Comet Hale-Bopp were obtained in the period 16-22 of April with the CoCAM wide-field imaging instrument on La Palma plus a narrow-band sodium filter ($\lambda_c = 5892\text{Å}$, FWHM= 15Å) designed to isolate emission from the sodium D₂ and D₁ lines. CoCAM consists of a 35mm camera zoom lens working at f/3.5 and imaging onto a 2220×1180 pixel EEV CCD chip, whose pixel size of 22.5μ m square corresponds to 26 arcsec, thereby achieving on the sky a total field of 17×9 degrees. Imaging was also obtained with filters designed to isolate both H_2O^+ emission in the ion tail ($\lambda_c = 6185\text{Å}$, FWHM= 42Å) and the solar continuum due to dust scattering ($\lambda_c = 6250\text{Å}$, FWHM= 25Å). The wide field sodium images immediately revealed the presence of a very linear structure stretching several degrees close to the anti-sunward direction, with no obvious counterpart in the H₂O⁺ and dust images, and which we took to be a separate neutral Na tail (Cremonese et al. 1997, Fitzsimmons et al. 1997). An example image is shown in figure 1. High-resolution spectroscopy was performed at several points along this tail on April 19.9 UT, 20.9 UT and 23.9 UT, using the 4.2m William Hershel Telescope with the Utrecht Echelle Spectrograph and 1024×1024 pixel TEK CCD chip, providing a dispersion of 0.053 Å pixel⁻¹ and a resolution of 0.1 Åwith a slit width of 1.1 arcsec. On the last date the narrow-band sodium filter described above was placed in the spectrograph, thereby allowing long-slit spectroscopy to be performed. This configuration allowed us to have a larger spatial coverage of 2.7 arcmin while simultaneously isolating the single order with only the NaD emission lines. In all spectra redshifted Na emission was observed, thereby confirming the presence of neutral sodium in this tail. Unfortunately it was not possible to obtain both images of the sodium tail and high resolution spectra in the long slit configuration during the same night, due to only one sodium interference filter being available. The comet during these nights had a heliocentric distance of 0.98 AU and a geocentric distance of 1.61 AU.

All the spectra were cosmic-ray cleaned and bias-subtracted using FIGARO spectroscopic reduction routines (Shortridge et al. 1997). For the normal echelle-mode data obtained on the 19th and 20th April, each order was individually flatfielded using tungsten lamp exposures at the same instrumental settings. Wavelength calibration was performed via exposures of a thorium-argon lamp obtained at the beginning and end of the period of visibility of the comet. From these arc-lamp exposures, the instrumental resolution in the order containing the NaD lines was 0.11Å FWHM. Due to the short length of the slit in this

observing mode necessary to avoid order overlap (3.2 arcsec), no flux calibration was attempted. Because of severe instrumental problems, comparison lamp exposures were not possible on the 23rd April. Therefore after bias subtraction and cosmic-ray removal, wavelength calibration was performed using the strong NaD airglow lines observed simultaneously with the cometary emission. Exposures of the lunar surface had the reflected solar spectrum removed, thereby leaving simply the transmission profile of the order isolating filter. This was then used to correct the data for the filter transmission profile at all points along the slit. Flux calibration for these data was obtained via exposures of the standard star BD +75°325 (Oke 1990) with a 7.0 arcsec wide slit. A representative spectrum is shown in figure 2.

3. Analysis and Discussion

From these spectra, the brightness and velocity as a function of distance along the tail has been modelled assuming that the gas was produced by the nucleus and/or a near–nucleus source with dimensions much smaller than the tail length. It then undergoes acceleration in the antisun direction due to simple radiation pressure, through photon scattering (fluorescence) in the resonant D-line transitions. In this case the column density of Na atoms at a sky–projected cometocentric distance L along the tail is equal to

$$N(\text{Na}) = \frac{Q(\text{Na})}{lv(L)} e^{-\frac{t}{(r_h^2 \tau)}}$$
(1)

where Q(Na) is the production rate, τ is the lifetime of the sodium atoms at a heliocentric distance of 1 AU, r_h is the heliocentric distance along the tail, l is the sky-projected linear dimension of the tail cross-section, v(L) is the sky-projected Na velocity along the tail, and t is the mean travel time of the Na atoms from the nucleus to the tail distance L. In the approximation of a purely antisunward sodium velocity, then the sky-projected sodium velocity v(L), the heliocentric sodium velocity v_h and the radial sodium velocity measured in the Echelle spectra v_E are related by $v(L) = v_h \sin \alpha$ and $v_E = \dot{\Delta} + v_h \cos \alpha$ where α is the phase angle and $\dot{\Delta}$ is the comet geocentric velocity. If v_0 is the starting velocity of the Na atoms from the source, then the width of the tail will be $l = 2v_o t + l_o$, where l_o is the linear dimension of the source region. Moreover, the transverse acceleration of the Na atoms due to the random-walk nature

of the scattering process should be taken into account. We find that Na atoms starting with an outflow velocity of $v_o \approx 1$ km s⁻¹ provides a width l close to that observed, and that the term $2v_0t$ dominates the others for $L > 10^7$ km. Then, the average emitted intensity (in rayleighs) of the tail axis is given by

$$I(\text{Na}) = 10^{-6} N(\text{Na}) \frac{g(L)}{r_h^2} = \frac{10^{-6} Q(\text{Na})}{2v_o t v(L)} \frac{g(L)}{r_h^2} e^{-\frac{t}{(r_h^2 \tau)}}$$
(2)

where g(L) is the photon scattering efficiency, or g-factor, in the D_1 and D_2 lines at 1 AU. As this region of the solar spectrum also displays several additional absorption lines, the g-factor is highly dependent on the heliocentric velocity and consequently on v(L) and L. Therefore the acceleration due to solar radiation pressure, assuming that emission out the D_1 and D_2 lines is negligible, is also dependent on the velocity and heliocentric distance, and allows us to compute the ratio between the radiation pressure force and the solar gravitational force;

$$\beta(\text{Na}) = \frac{h \ g(L)(1 \ AU)^2}{\lambda GM_{\odot}m}$$
 (3)

where G is the gravitational constant, h is Planck's constant, M_{\odot} is the Sun's mass and m is the mass of the Na atom.

Figure 3 shows the g(L) factor, the $\beta(Na)$ factor, the modelled and observed tailward velocities and surface brightness along the tail. Surface brightnesses were measured from the spectra rather than the CoCAM data due to large uncertainties resulting from attempts to accurately calibrate these extremely wide-field images. The lifetime for photoionization of the sodium atom is rather controversial. Using measurements of the Na cross section by Hudson and Carter (1967), Huebner et al. (1992) evaluated an experimental lifetime of $\tau = 6.17 \times 10^4$ s at a heliocentric distance of 1 AU. However, following a theoretical recalculation of the cross section by Chang and Kelly (1975), Huebner et al. also suggested a value almost three times longer of $\tau = 1.69 \times 10^5$ s. In previous studies of the Moon, Mercury, Io and other comets, values close to the shorter "experimental" Na lifetime quoted above have been used. However, Killen et al. (1997) have claimed to require a longer lifetime to explain the different accommodation time of the sodium atoms on the surface of Mercury and some characteristics of its atmosphere. Therefore we attempted to fit the observed brightness distribution assuming both of the above photoionization timescales. As shown in figure

3, the observed brightness of the tail is consistent with our model if we adopt the longer photoionization timescale of $\tau = 1.69 \times 10^5 \ s$ at 1 AU.

Modelling has also been applied to the CoCAM images, again assuming that radiation pressure due to resonance fluorescence in the D-lines is solely responsible for the existence of the tail. If the particles with the same β are ejected with velocity v_0 from the inner coma, then the resulting Na tail will be a syndynamic tube of width $2v_0t$. The axis of this syndynamic tube is the *syndyne* defined by $\beta(Na)$, which is computed by means of Keplerian mechanics (Finson and Probstein 1968, Fulle 1992). Applying the syndynamic model to CoCAM images taken on April 21.9 UT and trying to fit the data with different values of β , Table 1 lists the Position Angles (PA) of the Na tail: PA_O is measured from the CoCAM images, and PA_C is the computed PA of the range of best fitting syndynes of $\beta = 100 \pm 20$. This high value of β implies that only atoms can satisfy the fit and not molecules or dust grains, for which the largest value reported in literature is $\beta \simeq 2$.

We applied the same syndynamic model to the D-line emission velocities measured within the sodium tail. In Table 2, those observed (v_{ro}) on April 23.9 UT are compared with those predicted from the model (v_{rc}) , assuming the best fitting $\beta=82\pm3$. This value is consistent with, but much more accurate than, that provided by the tail PA fit. We stress that such a high β value would be impossible for dust particles, but is entirely reasonable for atoms. Using this value in equation (3) we deduce $g/m=0.72\pm0.03~{\rm s}^{-1}$ amu⁻¹. Since for sodium at 1 AU $g\leq15.6~{\rm s}^{-1}$, we calculate the mass of any possible sodium-bearing molecule in the tail as $m\leq22\pm1$ amu. This conclusively demonstrates that the observed tail is composed of neutral Na atoms alone, as Na-bearing molecules would then be too massive to be consistent with such a high β ratio. The excellent fit between theory and observations, provided by both models, allows us to conclude with large confidence that the observed Na tail is due to fluorescence of Na atoms which have been released from the nucleus and/or a near-nucleus source and not in-situ in the sodium tail.

The data presented here do not reveal the exact nature of the source of the sodium atoms observed in the tail. From the absolute flux calibration of the spectra on April 23.9 UT, we obtain a production rate of $Q(\text{Na}) \simeq 5 \times 10^{25} \text{ atoms s}^{-1}$. The water sublimation rate at this time was of order $\sim 1 \times 10^{31}$ molecules s^{-1} (Dello Russo et al. 1997). Assuming that Hale-Bopp possessed normal cosmic abundances with Na/O = 2.4×10^{-3} (Anders and Grevesse 1989), then $\sim 0.1\%$ of the sodium in the comet was being released into the tail at this time. Furthermore the percentage of visible sodium could be altered by a factor 2 or more if

we take into account the very large dust-to-gas ratios mentionned for Hale-Bopp and the likely significant O content in the refractory dust. In any case this implies that whatever the source, the majority of Na remained unobservable in this comet.

4. Conclusions

We have reported both imaging and high-resolution spectroscopy of the sodium tail associated with comet C/1995 O1 Hale-Bopp. Two different approaches have been used to analyze the new sodium tail which allow the identification of the mechanism responsible; the simple but effective process of fluorescence. Based on this mechanism, we expect the appearance of a sodium tail to vary strongly with observing geometry (phase angle) and heliocentric velocity of the comet as the Na emissions move with respect to the solar Fraunhofer absorption lines (the Swings effect), thereby changing their intensity and acceleration. This is therefore a possible explanation for the different Na distributions observed in Hale-Bopp at other dates (Wilson et al. 1997) and in previous comet observations.

The associated modelling supports the theoretical value for the photoionization lifetime of the sodium atom of $\tau = 1.69 \times 10^5~s$ at 1 AU, a factor 3 higher than that generally used to study the exospheres of other Solar System bodies, e.g. the Moon and Io. The tail sodium atoms appear to have been released in the near-nucleus region of the comet, and not in-situ via the break-up of Na-bearing molecules, ions or dust particles. Assuming normal cosmic abundances for the comet, $\sim 0.1\%$ of the expected amount of sodium released by the comet is directly observable in the Na tail. Both future analysis of existing data and observations of other comets should concentrate on investigating the exact source distribution in the inner coma.

REFERENCES

Anders, R. & Grevesse, E., 1989, Geochim. Cosmochim. Acta, 53, 197.

Cremonese, G. & The European Hale-Bopp Team, 1997, IAU Circ., 6631.

Chang, J.-J. & Kelly, H.P., 1975, Phys. Rev. A, A12, 92.

Dello Russo M., Mumma, M.J., DiSanti, M.A., Magee-Sauer, K., Novak, R., Rettig, T., 1997 IAU Circ., 6682.

Finson, M.L. & Probstein, R.F., 1968, ApJ, 154, 327.

Fitzsimmons, A. & Cremonese, G. & The European Hale-Bopp Team, 1997, IAU Circ., 6638.

Fulle, M., 1992, A&A, 265, 817.

Hicks, M.D. & Fink, U., 1997, Icarus, 127, 307.

Hudson, R.D. & Carter V.L., 1967, J.Opt.Soc.Am., 57, 651.

Huebner, W.F., 1970, A&A, 5, 286.

Huebner, W. F., Keady, J. J., & Lyon S. P., 1992, Ap&SS, 195, 1.

Jessberger E.K. & Kissel, J., 1991, in Comets in the Post-Halley Era, 1075.

Killen, R.M., Potter, A.E., Morgan, T.H., 1997, BAAS, 29, 987.

Newall H.F., 1910, MNRAS, 70, 459.

Nguyen-Huu-Doan, 1960, Journal des Observateurs, 43, 61.

Oke, J.B., 1990, AJ, 99, 1621.

Rahe J., McCracken C.W., Donn B.D., 1976, A&ASuppl., 23, 13.

Shortridge, K, Meyerdicks, H., Currie, M., Clayton, M., Lockley, J., 1997, FIGARO version 5.2-0b User's Guide.

Sivaraman, K.R., Babu G.S.D., Bappu M.K.V., Parthasarathy M., 1979, MNRAS, 189, 897.

Spinrad, H. & Miner, E.D., 1968, ApJ, 153, 355.

Thomas, N., 1992, Surveys in Geophys., 13, 91.

Wilson, J.K., Mendillo, M., Baumgardner, J., 1997, BAAS, 29, 1047.

We gratefully acknowledge the staff of the Isaac Newton Group who built and operated the CoCAM. The William Herschel Telescope is operated on the island of La Palma by the Royal Greenwich Observatory in the Spanish Observatorio del Roque de los Muchachos of the Instituto de Astrofisica de Canarias. This project has been supported by the European Commission through the Activity "Access to Large-Scale Facilities" within the Programme "Training and Mobility of Researchers", awarded to the Instituto de Astrofisica de Canarias to fund European Astronomers' access to its Roque de Los Muchachos and Teide Observatories (European Northern Observatory), in the Canary Islands. We further thank M.Mendillo and J.Baumgardner for the use of their sodium interference filter and their useful suggestions on the observations.

This manuscript was prepared with the AAS IATEX macros v4.0.

Fig. 1.— Images of Comet Hale–Bopp obtained with CoCAM and the narrow–band Na and H_2O^+ filters on April 16.9 UT. The image is composed by two square picture with each linear dimension spanning 7.4 degrees, or 3.1×10^7 km at the comet nucleus. The neutral sodium tail described in the text is seen as a linear feature to the left of the left picture and distinct from the normal and more diffuse dust tail on the right. The continuum image has not been subtracted in either image in order to show clearly that all three tails are distinct from one another.

Fig. 2.— Spectrum of the sodium tail 3.1 degrees from the nucleus of Hale-Bopp, obtained with the WHT plus Utrecht Echelle Spectrograph on April 23.9 UT. Sky lines due to OH and Na are labelled. The cometary Na D-lines are clearly observable due to an apparent Doppler shift of 144 km s⁻¹ from the terrestrial sky emission.

Fig. 3.— (a) Theoretical g factors for the D_1 line (bottom), D_2 line (middle), and both combined (top)as a function of the tail distance deprojected along the antisolar direction. (b) β (Na) values in function of the Tail Distance deprojected along the antisolar direction. (c) Measured velocities (*), deprojected along the antisolar direction, compared to the computed velocity (curve). (d) Observed brightness distribution in the tail as measured from the high-resolution spectra versus model predictions for two photoionization lifetimes: 1) (lower) assuming a Na lifetime at 1 AU of $\tau = 14$ hours (the experimental photoionization cross section) and 2) (upper) assuming $\tau = 47$ hours (theoretical photoionization cross section).

Table 1. Position angles obtained with the syndynamic model

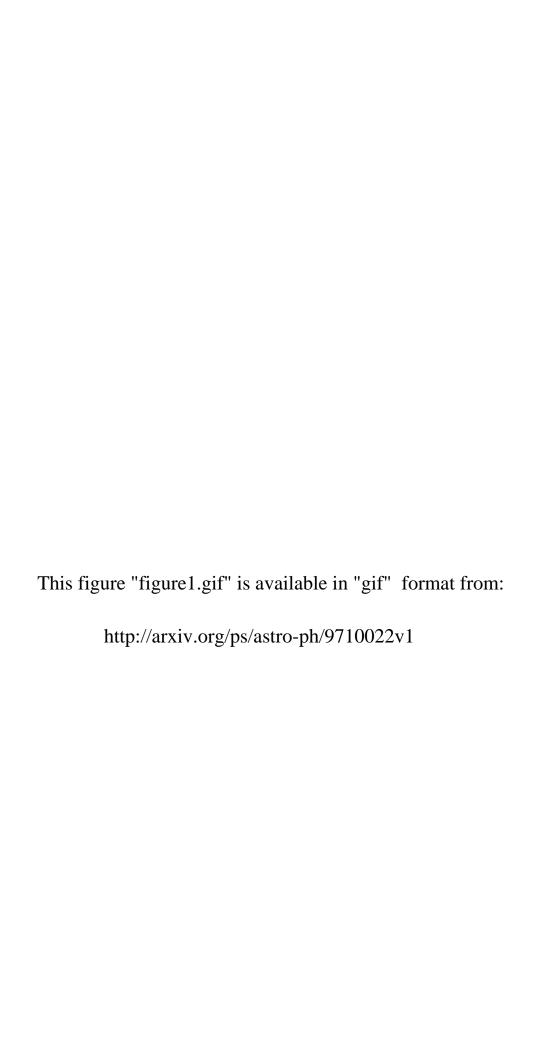
L	L	PA_O	PA_C
deg	$10^6~\mathrm{km}$	\deg	\deg
1.33	5.6	61.9 ± 1.0	59.8 ± 0.5
2.11	8.9	$59.2 {\pm} 0.8$	$58.8 {\pm} 0.5$
2.70	11.4	$59.0 {\pm} 0.7$	$58.2 {\pm} 0.5$
3.78	16.0	$57.1 {\pm} 0.6$	57.0 ± 0.5
4.66	19.7	$55.6 {\pm} 0.5$	56.0 ± 0.5

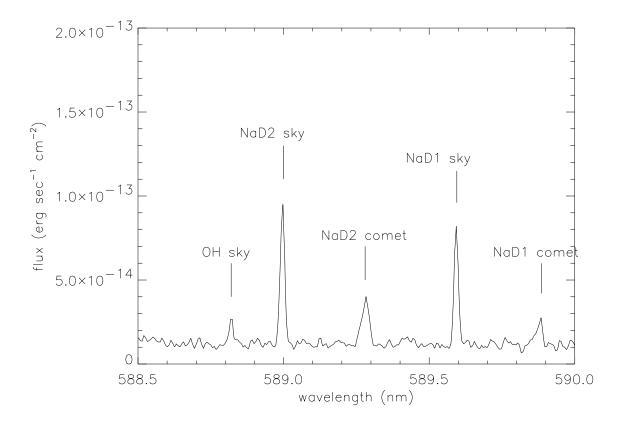
Note. — Observed position angles PA_O for the Na tail as a function of the sky-projected distance L from the nucleus on April 21.9 UT, compared to those calculated PA_C from the syndynamic model discussed in the text, with $\beta = 100 \pm 20$. Note that the model underestimates the observed PA close to the comet nucleus: to fit these values, larger β (i.e. larger g factors) would be required. However, close to the nucleus the PA_O measurements are affected by the largest errors, due to the Na tail width.

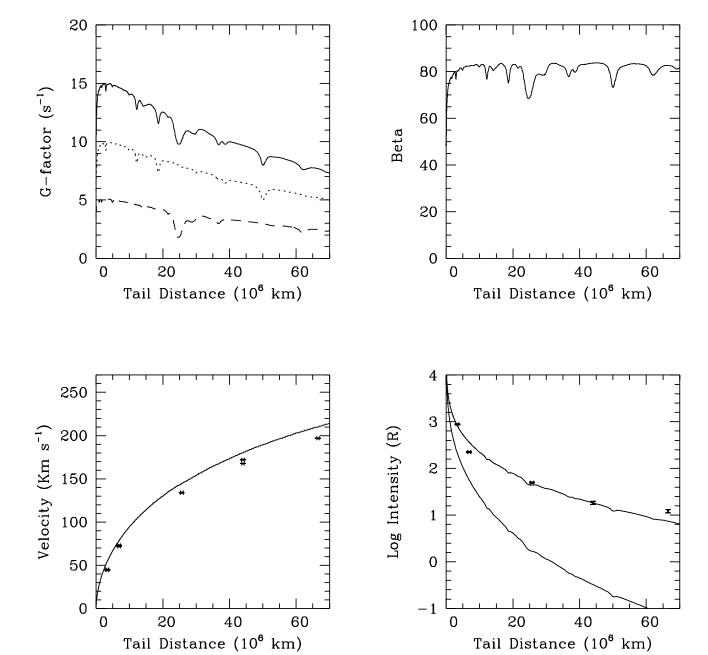
Table 2. Velocities along the sodium tail.

L deg	$ m L$ $10^6~{ m km}$	$ m v_{ro}$ $ m km~s^{-1}$	$ m v_{rc}$ $ m km~s^{-1}$	t days
0.89	3.83	62±1	63±2	2.0 ± 0.1
3.13	13.49	$117{\pm}1$	118 ± 2	3.7 ± 0.1
5.07	21.89	$149{\pm}1$	151 ± 3	5.0 ± 0.1
7.17	31.03	178 ± 1	176 ± 3	6.1 ± 0.1

Note. — Observed and modelled velocities in the sodium tail on April 23.9 UT. L is the sky-projected distance from the nucleus, v_{ro} is the measured radial velocity corrected for the relative velocity between comet nucleus and Earth, v_{rc} is the computed radial velocity of the Na atoms along the line of sight in the comet nucleus reference frame (to be compared directly with v_{ro}) for the best fitting syndyne of $\beta = 82 \pm 3$, t is the travel time of the Na atoms from nucleus to tail distance L.







Tail Distance (10⁶ km)